ELSEVIER

Nuclear Instruments and Methods in Physics Research A 458 (2001) 55–61

NUCLEAR INSTRUMENTS & METHODS IN PHYSICS RESEARCH Section A

www.elsevier.nl/locate/nima

Preliminary performance of CdZnTe imaging detector prototypes

B. Ramsey[a], D.P. Sharma[a], R. Austin[a], V. Gostilo[b,*], V. Ivanov[b], A. Loupilov[b], A. Sokolov[b], H. Sipila[c]

[a]*Space Science Department, Marshall Space Center, Huntsville, AL 35812, USA*
[b]*Baltic Scientific Instruments, Ganibu dambis 26, P.O. Box 33, LV-1005 Riga, Latvia*
[c]*Metorex International Oy, Nihtisillankuja 5, FIN-02631 Espoo, Finland*

Abstract

The promise of good energy and spatial resolution coupled with high efficiency and near-room-temperature operation has fuelled a large international effort to develop cadmium–zinc–telluride (CdZnTe) for the hard-X-ray region. We present, here, preliminary results from our development of small-pixel imaging arrays fabricated on $5 \times 5 \times 1$-mm and $5 \times 5 \times 2$-mm spectroscopy and discriminator-grade material. Each array has 16 (4×4) 0.65-mm gold readout pads on a 0.75-mm pitch, with each pad connected to a discrete preamplifier via a pulse-welded gold wire. Each array is mounted on a three-stage Peltier cooler and housed in an ion-pump-evacuated housing which also contains a hybrid micro-assembly for the 16 channels of electronics. We have investigated the energy resolution and approximate photopeak efficiency for each pixel at several energies and have used an ultra-fine beam X-ray generator to probe the performance at the pixel boundaries. Both arrays gave similar results and at an optimum temperature of -20°C we achieved between 2% and 3% full-width at half-maximum energy resolution at 60 keV and around 15% at 5.9 keV. We found that all the charge was contained within one pixel except very close to the pixels edge, where it would start to be shared with its neighbor. Even between pixels, all the charge would be appropriately shared with no apparently loss of efficiency or resolution. Full details of these measurements will be presented, together with their implications for future imaging-spectroscopy applications.

Keywords: Imaging arrays; Pixel detectors

1. Introduction

The many advantages of a high-atomic-number, near-room-temperature semiconductor has led to the development of cadmium–zinc–telluride (CdZnTe) for many applications in medicine, engineering and science as well as for space projects.

For astrophysical applications, a test 4×4 pixel CdZnTe detector of dimensions $10 \times 10 \times 5$ mm has been developed in Ref. [1]. Here, the pixel size was 1.5 mm with an inter-pixel distance of 0.2 mm. Typical energy resolutions of 7%–10% were achieved at 60 keV (^{241}Am) for an uncollimated beam, and this dropped to around 4% when collimation was applied.

* Corresponding author. Tel.: +371-738-3947; fax: +371-735-3677.
E-mail address: bsi@bsi.lv (V. Gostilo).

0168-9002/01/$ - see front matter
PII: S0168-9002(00)00851-2

In Ref. [2], a detector with a crystal size of $10 \times 10 \times 2$ mm having 4×4 pixels each of 1.5 mm^2 was developed. The average energy resolution obtained on the pixels was 4.4%, with a best result of 3.3% at 60 keV.

In this work, we report the results of arrays with finer pixels. These are being developed for the focus of a hard-X-ray telescope under construction for astronomical observations [3]. The plate scale of the telescope necessitates sub-millimeter spatial resolution in the focal-plane detector, coupled with a "large" overall area, 20 mm × 20 mm to cover the instruments full field-of-view. The arrays reported here and elsewhere [4] are the necessary first step towards achieving that goal.

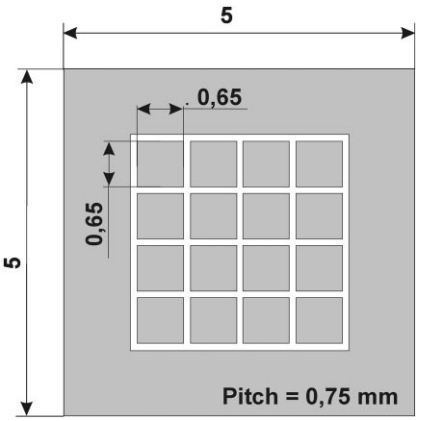

Fig. 1. Layout of 4×4 pixel detector.

2. Pixel-detector fabrication

We have developed and fabricated small-pixel imaging detectors using CdZnTe crystals of dimensions $5 \times 5 \times 1$ mm and $5 \times 5 \times 2$ mm. These were of both certified spectroscopy and discriminator grade and were delivered by eV products such as plane parallel detectors with gold contacts.

In the final configuration, each detector has 16 (4×4) readout pads with dimensions 0.65×0.65 mm on a 0.75 mm pitch, as shown in Fig. 1. The 16 pixels were surrounded by a guard ring, which was extended to the edge of the crystal. The purpose of this guard ring was to reduce the influence of surface leakage currents, and preserve continuity of field so that charge collection for edge pixels would be the same as that for interior ones.

Before pixel-detector fabrication, we performed quality control on the crystals by measuring the current–voltage (I–V) characteristics, their mobility-lifetime products, energy resolutions at 59.6 keV [5]. For manufacture of pixel detectors, we further selected only crystals whose characteristics were stable with time.

Typical crystals have inclusions, crystalline borders and twins that can considerably degrade their performance as pixellated detectors. Therefore, the crystals with the least number of borders and twins were selected for the manufacture of pixel detectors. These were determined by visual inspection after the original planar electrodes were removed.

The new pixel contact pads were fabricated using photolithography and gold deposition from chloroauric acid. To provide good spectroscopic performance, the detectors should have contact pads that assure a low current leakage level and high interpixel resistivity, do not introduce additional noise, and that are stable with time. The other important requirement is that the contact pad should have good mechanical strength to permit connection to the readout electronics.

With this in mind, we have used a modified technology for the manufacture of the contact pads [5]. The conventional process fabricates anode and cathode contacts by gold or platinum deposition at the chemically etched crystal surface. However, in our case, the cathode was manufactured by this technology, but the anode pads were made by gold deposition on to a mechanically polished surface. It is known that mechanical damage of the crystal surface of p-type CdTe causes a conductivity inversion, so that a mechanically damaged layer at the crystal surface could have an n-type conductivity. The structure gold–(p-CdTe)–(n-mechanically damaged surface)–gold then works as a p–n barrier. Fig. 2 shows I–V characteristics of such CdTe structures compared with ordinary ones. The presence of the p–n barrier causes some reduction of the reverse leakage current. We suppose that the same process might take place with CdZnTe crystals. As delivered, the CdZnTe crystals had a weak p-type conductivity.

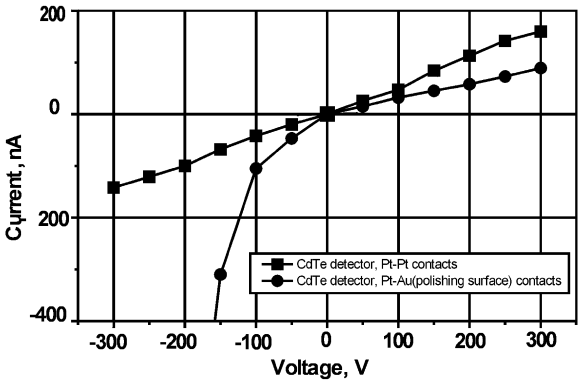

Fig. 2. Current–voltage characteristics for detectors with different contacts.

The use of polished crystal surfaces allows the contact pads to be made by traditional methods to provide pads that are relatively insensitive to mechanical damage and have improved mechanical strength. Side-by-side spectroscopic performance comparisons on the same crystal have demonstrated the superior performance of the polished surface contacts. These contacts appear very stable with no evidence of change of operating characteristics with time.

3. Experiment

The fabricated pixel detectors were installed on the Al_2O_3 dielectric substrate of the hybrid microassembly which contained 16 discrete-input-stage low-noise charge-sensitive preamplifiers with resistive feedback ($R_f = 1\,G\Omega$) and thermosensor [6].

In the center of the substrate is a square hole, 3.5×3.5 mm size, which is less than the full area of the detector crystal (5×5 mm). Around the hole there is a metallized pad for electrical contact. The detector was glued to the contact pad with conductive adhesive, with the sensitive volume above the hole in the substrate (Fig. 3). Such a configuration permits the detector to be irradiated from the cathode side and the anode connections to be made to the preamplifiers. Wire bonding between the detector pads and the inputs to the preamplifiers was made by pulse welding using gold wire 30 μm in diameter.

The hybrid microassembly with the pixel detector was installed at the cold side of a Peltier cooler inside a vacuum chamber (Fig 3) equipped with a Be window for detector irradiation. A three-stage Peltier cooler (10 W) gave a useful temperature range from ambient down to $-40^{\circ}C$. A miniature sputter ion pump was installed inside the chamber to maintain the necessary vacuum.

Signals from the 16 input stages were routed through a vacuum connector to the main amplification and temperature-stabilization unit. From there they were fed into standard rack spectroscopic equipment for amplification and shaping. All supply voltages (high voltages for detector and for the magnetic pump, and low voltages for the Peltier cooler and electronics), as well as temperature monitoring and control (to $\pm 0.1^{\circ}C$ was provided via a universal supply unit.

4. Results

4.1. General comments

The CdZnTe crystals were delivered to us as plane-parallel certified spectroscopy and discriminator grade detectors with gold contacts. During fabrication and testing, we did not find any difference between the performance of pixel detectors fabricated from these two materials.

Pixel leakage currents at room temperature and an operating voltage of 200 V did not exceed 0.5–0.8 nA with all fabricated detectors. The inter-pixel resistance with all manufactured detectors was in the range 4×10^{10}–$3 \times 10^{11}\,\Omega$.

The spectrometric characteristics of the 2-mm-thick pixel detector were marginally better than the 1-mm-thick device. It might be expected that the thicker crystal would perform significantly better, particularly at higher energies (60 keV and above), as the greater thickness to X-ray penetration ratio would reduce tailing. Further, the smaller pixel capacitance due to the greater thickness should lead to some reduction of the capacitance noise. These benefits were not really evident from the data.

The effects of operating temperature were investigated on each array. Optimum results were ob-

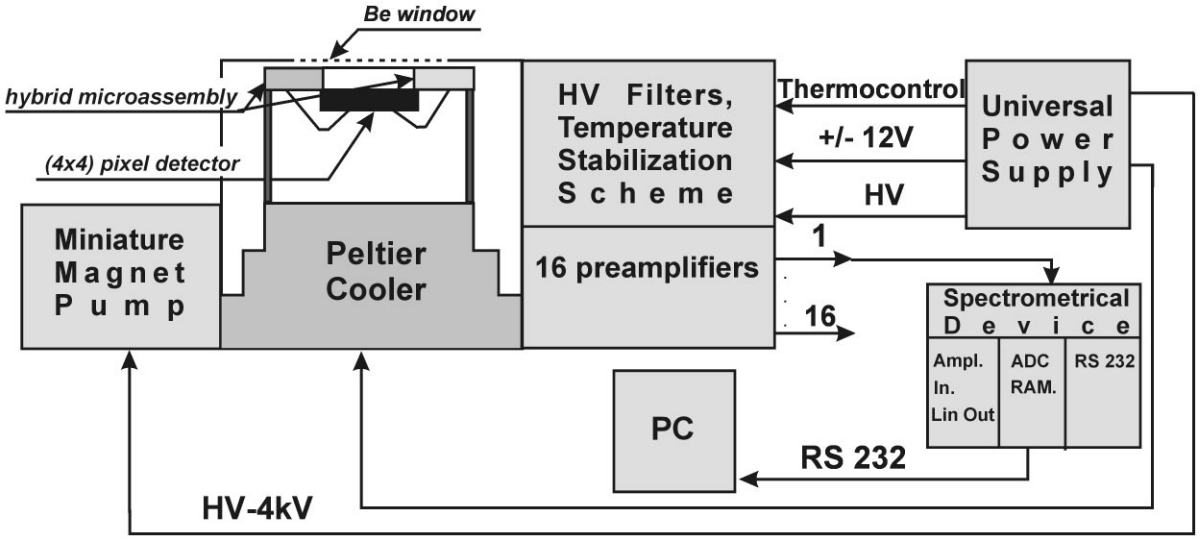

Fig. 3. Experimental schematic (under development).

tained for an operating temperature of around -20°C. This temperature was used for all of the tests explained in detail below.

4.2. 1-mm thick detector array

4.2.1. Energy resolution

We have measured the energy resolution of each pixel at three energies, while operating the array at an optimum temperature of -20°C. These data are given in Fig. 4. It can be seen that there is good uniformity between pixels and that on an average the resolutions were just over 2% full-width at half-maximum (FWHM) at 60 keV, around 5% at 22 keV and 17% at 5.9 keV. These results were obtained by irradiating the whole array and taking data from each single pixel in turn. Thus they contain a portion of events where the charge is shared with neighbouring pixels (see Section 4.2.3), giving a tail on the low-energy side of each photopeak. Running adjacent pixels in anticoincidence, or collimating the beam to irradiate just the central portion of each pixel, would give a slight improvement to the resolutions quoted above.

We have employed the anticoincidence technique to examine the photopeak to continuum ratio for four typical pixels in the array. We have

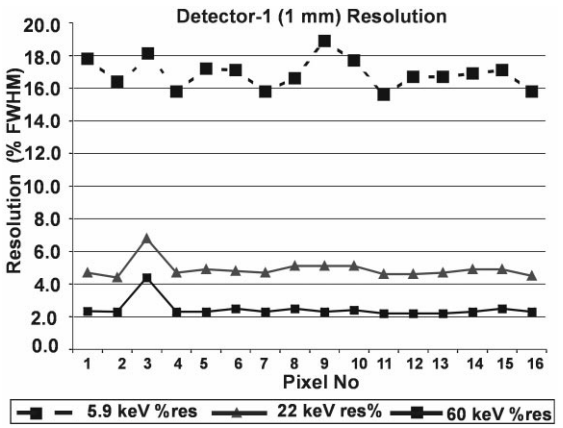

Fig. 4. Pixel energy resolution at 5.9, 22.2 and 59.6 keV for the 1-mm-thick detector array.

found that at 60 keV approximately 70% of the events reside in the photopeak, which we have somewhat arbitrarily defined as having a width of $2\times$ the FWHM resolution at 60 keV.

4.2.2. Stability

Two areas of concern with CdZnTe detectors are their stability with time and their overall charge-collection efficiency, particularly at low energies

where the events are absorbed very close to the crystal surface. We find no statistically significant variations in gain or charge-collection efficiency over a 24 h operating period and have checked the array at 6 keV against a silicon detector to gauge absolute efficiency at this energy. The CdZnTe array was found to give a count rate 3% lower than the silicon detector with a 1 sigma error of 1%.

4.2.3. Scans across individual pixels

A finely collimated ($< 100\,\mu m$) 8 keV (Cu K_α) X-ray beam has been used to probe any non-uniformities within individual pixels and to examine behaviour in the interpixel gaps. Fig. 5 shows the results for a typical pixel. Here, the total counts, continuum counts and the photopeak counts are plotted as a function of beam position across the pixel. It is evident that the active size of the pixel matches its geometric size and that within the pixel, the response is very uniform. The counts in the continuum curve are seen to rise at each end near the edges of the pixel. This is due to charge sharing between this and the adjacent pixel which removes counts from the photopeak and adds them to the continuum.

4.2.4. Recovery of events from the interpixel gaps

To investigate if charge is lost between pixels, we have scanned the X-ray beam across three adjacent pixels (numbers 9, 12 and 14), summed the pixels, and measured the total count rate and the energy

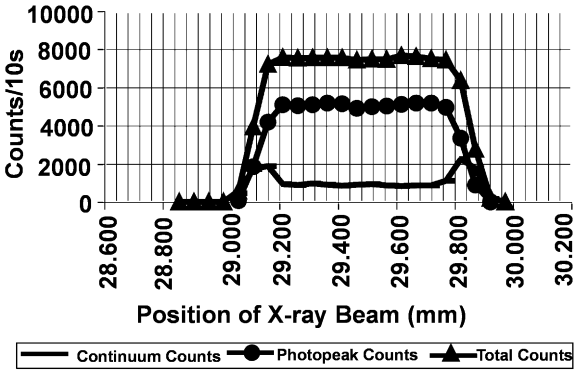

Fig. 5. Fine X-ray beam scan across an individual pixel for the 1-mm-thick detector array.

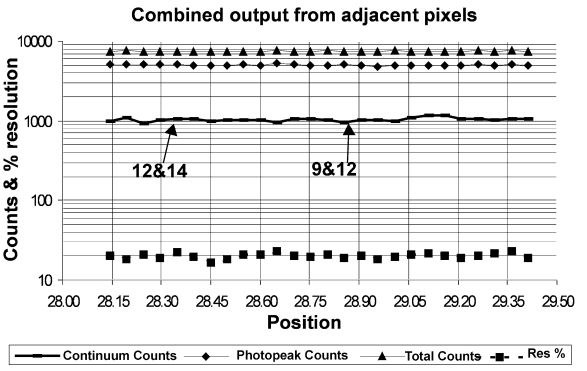

Fig. 6. Combined output from adjacent pixels (#9, 12, 14) as a function of collimated X-ray beam position for the 1-mm-thick detector. No signal loss is observed between pixels (see arrows).

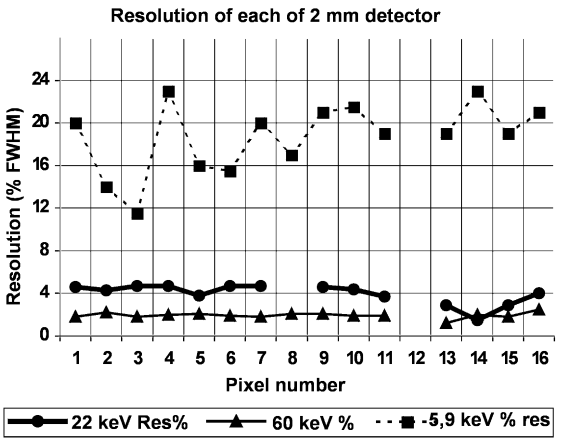

Fig. 7. Pixel energy resolution at 5.9, 22.2 and 59.6 keV for the 2-mm-thick detector array.

resolution as a function of position. These data are shown in Fig. 6, where a pair of arrows indicates the mid-point between pixels 9 & 12 and 12 & 14. It is evident from the figure that the data are continuous across the interpixel gaps and that full recovery can be obtained by adding together the charges that are shared between pixels.

4.3. 2-mm thick detector array

At present, the bulk of the data has been taken with the 1-mm-thick detector and the characterization

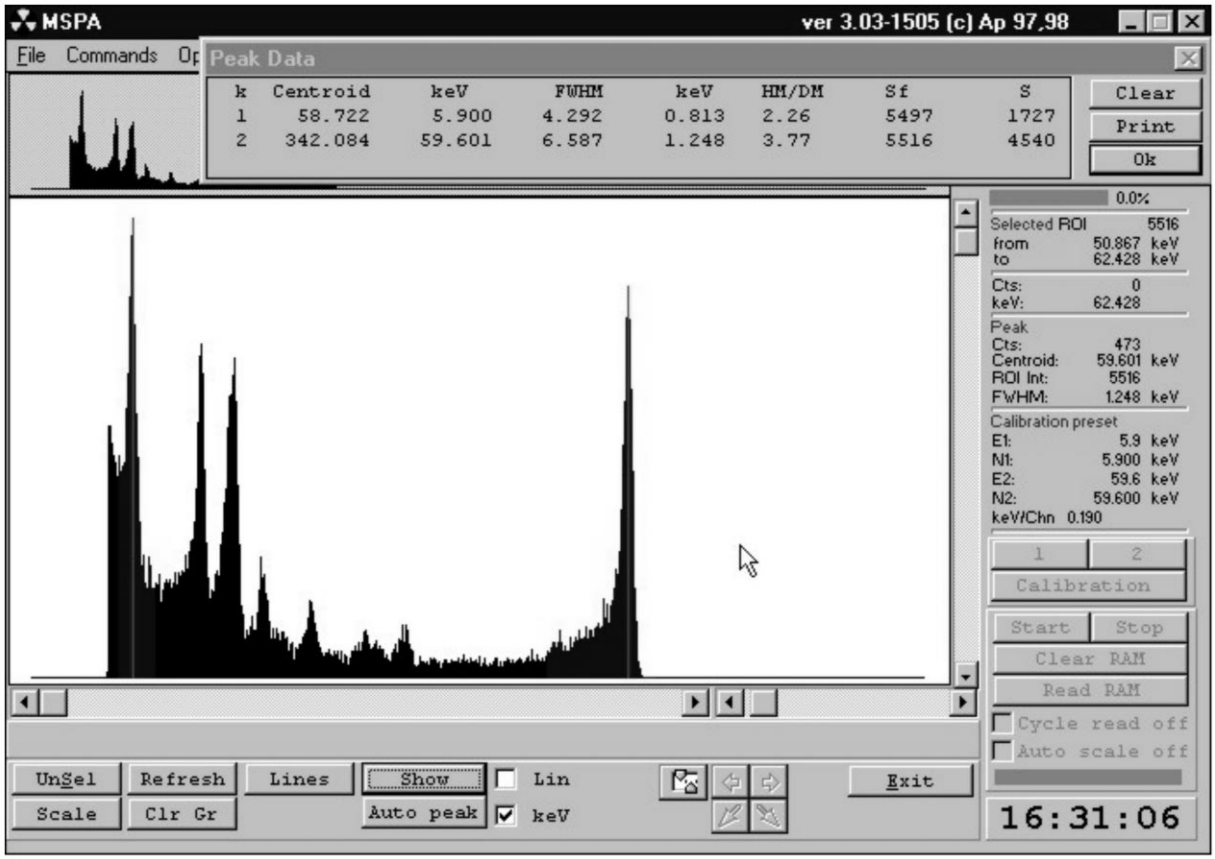

Fig. 8. Energy spectrum (^{241}Am + ^{55}Fe) for pixel 13 of the 2-mm-thick detector at a temperature of -20°C.

of the 2-mm unit has only just begun. Fig. 7 shows measurements of the energy resolution at three energies for each pixel in the 2-mm-thick array operated with 900 V bias and at a temperature of -20°C. Pixel 12 became noisy and no data were taken for it. For the remaining pixels, we once again obtained good resolutions and high uniformity. Preliminary tests with the collimated X-ray beam indicated non-uniform response within some pixels and these effects are currently being investigated. Other than this, the thicker array gave good response and excellent spectra, as can be seen from Fig. 8 which shows a detailed spectrum obtained by irradiating pixel 13 with both ^{55}Fe and ^{241}Am.

5. Conclusion

We have developed CdZnTe arrays with small pixels as a first step towards a large imaging array for astronomy. We find that the small arrays operate in a stable manner and give excellent spectroscopic results (around 2% at 60 keV). For the 1-mm-thick device, we find that charge sharing between pixels is limited to events in the interpixel gap only and that these events can be fully recovered by adding the signals from adjacent pixels. At low energies (6 keV), the 1-mm-thick device appears to be near 100% efficient and at high energies (60 keV), we measure a photopeak containing approximately 70% of all events.

Future work will comprise the continued evaluation of the 2-mm-thick array and, as a consequence of the encouraging results till date, the development of a larger area device with ASIC-type readout.

References

[1] P.E. Bloser, T. Narita, J.E. Grindlay, K. Shah, Semiconductors for Room-Temperature Radiation Detectors Application II, Vol. 487, Material Research Society, Warrendale, PA, p. 153.
[2] R. Sudharsanan, C.C. Stenstrom, P. Bennett, G.D. Vakerlis, Semiconductors for Room-Temperature Radiation Detectors Application II, Vol. 487, Material Research Society, Warrendale, PA, p. 245.
[3] B.D. Ramsey, D. Engelhaupt, C.O. Speegle, S.L. O'Dell, R.A. Austin, J.J. Kolodziejczak, M.C. Weisskopf, Proc. SPIE 3765 (1999) 822.
[4] D.P. Sharma, B.D. Ramsey, J. Mesiner, R.A. Austin, H. Sipila, V. Gostilo, V. Ivanov, A. Loupilov, A. Sokolov, Proc. SPIE 3765 (1999) 832.
[5] V. Gostilo, V. Ivanov, S. Kostenko, I. Lisjutin, A. Loupilov, S. Nenonen, H. Sipila, K. Valpas, Proceedings of 2000 IEEE Nuclear Science Symp. and Medical Imaging Conference, Lyon, France, October 15–20, 2000, to be published.
[6] V. Gostilo, Nucl. Instr. and Meth. A 322 (1992) 566.